

We are IntechOpen, the world's leading publisher of Open Access books Built by scientists, for scientists

6,900

Open access books available

186,000

International authors and editors

200M

Downloads

Our authors are among the

154

Countries delivered to

TOP 1%

most cited scientists

12.2%

Contributors from top 500 universities



WEB OF SCIENCE™

Selection of our books indexed in the Book Citation Index
in Web of Science™ Core Collection (BKCI)

Interested in publishing with us?
Contact book.department@intechopen.com

Numbers displayed above are based on latest data collected.
For more information visit www.intechopen.com



Variations in the Aerosol Optical Depth Above the Russia from the Data Obtained at the Russian Actinometric Network in 1976–2010 Years

Inna Plakhina

Additional information is available at the end of the chapter

<http://dx.doi.org/10.5772/48618>

1. Introduction

Investigation results of the atmospheric aerosol over the Russia territory are of great interest for the ecology and climate developments. The regularities of spatial and temporal variations in the Aerosol Optical Depth (AOD) and Air Turbidity Factor (T) can be received by the Russian actinometric network data (RussianHydrometeorologicalResearchCenter). Our analysis will be based on the “Atmosphere Transparency” special-purpose database created at the Voeikov Main Geophysical Observatory (MGO) on the basis of observational actinometric data. Author has many years cooperation with MGO in the region of the processing and analysis of these observation data. The relationship between the increases in the global surface air temperature and in the atmospheric content of greenhouse gases has been proven. The warming over the past 50 years has mainly been related to human activities (IPCC, Climate Change 2001, 2007). Along with the anthropogenic factor, climate is affected by such natural factors as variations in the solar constant, cyclic interactions between the atmosphere and the ocean, and atmospheric aerosol; these factors are pronounced within time intervals of several years to several decades. The sign of aerosol forcing may be different: the stratospheric aerosol layer causes the reflection of solar radiation incident upon the atmospheric upper boundary and, thus, decreases the warming of the underlying air layers. For example, the sulfate aerosol which formed in the stratosphere after the Pinatubo eruption (June 1991) caused “short” (in 1993) global cooling. Tropospheric aerosol can increase or decrease the surface air temperature, and its influence on the ecological state of the air is well understood (Isaev, 2001). Therefore, monitoring the atmospheric aerosol component is important and necessary now from the standpoints of its

climatic forcing and ecology. The study of current spatiotemporal variations in the atmospheric aerosol component is of scientific interest and presents a problem. Current ground-based networks of monitoring (in particular, AERONET) are the results of such interest (Holben et al., 1998). There are eight AERONET stations in Russia; seven of them are located in Siberia [8]. The maps, which show a global distribution of the sources of different anthropogenic, natural, organic, mineral, marine, and volcanic) aerosols arriving in the atmosphere, the total aerosol optical depth in the atmospheric thickness according to model data (IPCC, Climate Change 2001) and the aerosol optical depth according to satellite (MODIS) monitoring (IPCC, Climate Change 2007), show Russia as a territory of decreasing aerosol optical depth (AOD) going from south to north. At the same time, Russia occupies the entire northeastern part of Eurasia (30°E – 180°E; 50°N – 80°N) and includes different climatic zones which differ in water content, air temperature, cloudiness, solar radiation flux incident upon the land surface, underlying surface, and air-mass circulation. In addition, the density of population and the degree of industrialization of different Russian regions are very inhomogeneous in space. In the studies (Plakhina et al., 2007, 2009) we have shown that an analysis of the AOD of a vertical atmospheric column can be made on the basis of observational data obtained at the Russian actinometric network, in particular, on the basis of data on the integral atmosphere transparency (P), because P variations are, to a great extent, determined by the aerosol component of the attenuation of direct solar radiation; other components of the attenuation (water vapor and other gases) have little effect on its time variations. Thus, on the basis of data on the homogeneous (calibrated against a single standard and obtained with a unified method) observational series of direct solar-radiation fluxes at the land surface and estimates of the integral (total and aerosol) transparency, it is possible to analyze variations in the AOD of a vertical atmosphere. Now we continue this analysis on the basis of an extended database (the number of stations – 53, and the period of observations – 1976 – 2010 years. Now we present the character of multiyear seasonal variations in AOD, the simplest statistical parameters (means, extrema, and variation coefficients) of spatial variations in AOD annual means, the “purification” of the atmosphere from aerosol over the past 15 years (1995–2010 y.y.). Also we compare the effects of the two natural factors (the global factor—the powerful volcanic eruptions in the latter half of the 20th century which resulted in the formation of a stratospheric aerosol layer—and the regional tropospheric factor—for example, the arrival of aerosol in the atmosphere due to tundra and forest fires) on AOD.

2. Russian actinometric network data

Fig. 1 gives a map showing the location of 53 actinometric stations of the Russian network (Makhotkina et al., 2005, 2007; Luts'ko et al., 2001) for which the AODs of vertical atmospheric columns were estimated for a wavelength of 0.55μ from the measured fluxes of direct solar radiation at land surface. These stations cover a large part of Russia and are located outside the zones of direct local anthropogenic sources of industrial and municipal aerosol emissions (suburbs, rural areas, uplands, etc.). In other words, the considered spatiotemporal variations in AOD are formed under the influence of natural factors: the

advection of air masses from the regions with an increased or decreased aerosol load, volcanic eruptions, and forest and tundra fires. In analyzing the 1976–2010 observational data, our goal was to obtain an averaged pattern of the spatial distribution of atmospheric aerosol over Russia and to compare this pattern with that of the global aerosol distribution which is presented in the IPCC third (modeling) and fourth (satellite data, MODIS) reports (IPCC, Climate Change 2001, 2007). In this case, the estimates obtained with our method supplement the international data on the model approximations and satellite monitoring of AOD. The advantages of our estimates are the great length of the series of actinometric observations under consideration (35 years), the universal methods of measurements and data treatment for all the stations, and the vast coverage area of Russia's large territory.



Figure 1. Layout of 53 actinometric stations whose data will be analyzed in the chapter. It is possible that the list of the observation stations will be increased up to 80 for the special estimations.

3. Empirical data and analysis procedure

The special-purpose Atmosphere Transparency database formed at the Main Geophysical Observatory makes it possible to analyze both the integral and aerosol transparencies of the atmosphere. The stations given in Fig. 1 were selected with consideration for the quality and completeness of the instrumental series. The integral air transparency :

$$P = (S/S_0)^{1/2} \tag{1}$$

Where S is the direct solar radiation to the normal-to-flux surface, reduced to the average distance between the Earth and the Sun and a solar altitude of 30° ; S_0 is the solar constant equal to 1.367 kW/m^2 . The Linke turbidity factor is unambiguously correlated with P :

$$T = \lg P / \lg P_i = (\lg S_0 - \lg S) / (\lg S_0 - \lg S_i) = -\lg P / 0.0433 \tag{2}$$

The AOD of the vertical atmosphere was calculated with a method specially developed and used at the MoscowStateUniversity meteorological observatory (Abakumova et al., 2006) with consideration for its limitations and errors:

$$\text{AOD} = \{\ln S - [0.1886w^{(-0.1830)} + (0.8799w^{(-0.0094)} - 1) / \sinh]\} / \{0.8129w^{(-0.0021)} - 1 + (0.4347w^{(-0.0321)} - 1) / \sinh\} \quad (3)$$

An index of the Angström spectral attenuation which depends on the size distribution of particles and the coefficient of particle reflection—is assumed to be equal to 1; S is the direct solar radiation reduced to the average distance between the Earth and the Sun, W/m^2 ; and w is the water content of the atmosphere, g/cm^2 . The conditions of observations at the stations, as a rule, correspond to the weather of an anticyclonic type (clear or slightly cloudy) when the Sun is not blocked by clouds.

4. Spatial variations in aerosol optical depth AOD

Table 1 gives the multiyear means and extrema of the annual values of AOD and the standard deviations from these means, which are averaged over the all 53 stations under consideration (pointed in Fig.1) for the two periods. It is seen that the AOD mean over all the stations and the entire observation period is equal to 0.14 and varies from 0.29 to 0.07, which is in good agreement with the spatial range of the AOD variations obtained from the satellite and model data (for the Russian region) that are given in the IPCC third and fourth reports (0.30–0.05).

Period	AOD		σ	Trend of AOD variations in over 10 years
1976 – 2010	Mean	0.14	0.04	-0.02
	Maximum	0.29		+0.02
	Minimum	0.07		-0.05
1995 – 2010	Mean	0.12	0.04	-0.01
	Maximum	0.22		+0.05
	Minimum	0.05		-0.06

Table 1. Multiyear means, maxima, minima, and standard deviations of the annual means of AOD over all stations in absolute units.

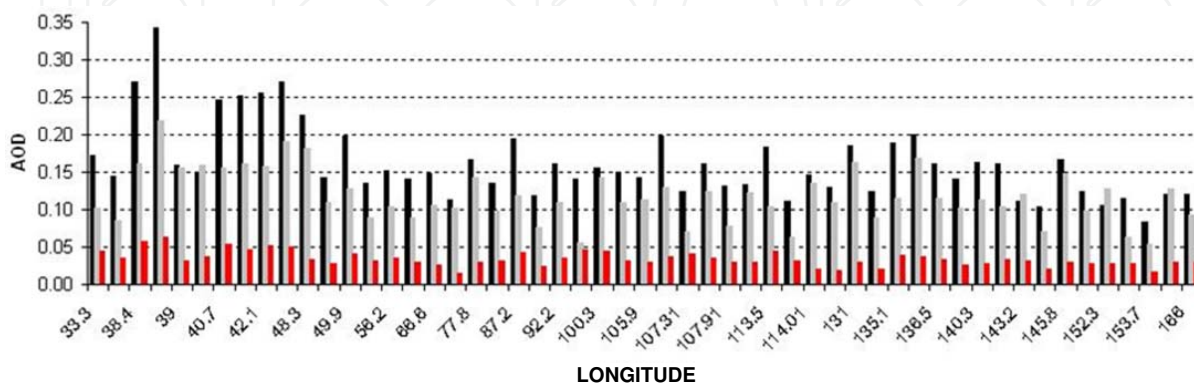


Figure 2. Statistics of the annual means of AOD for each of the stations: the ratio of the AOD means (black) over the period 1976–1994 and the AOD means (grey) over the period 1995–2010 and the standard deviations (red) in the series of the annual values of AOD for each of the stations.

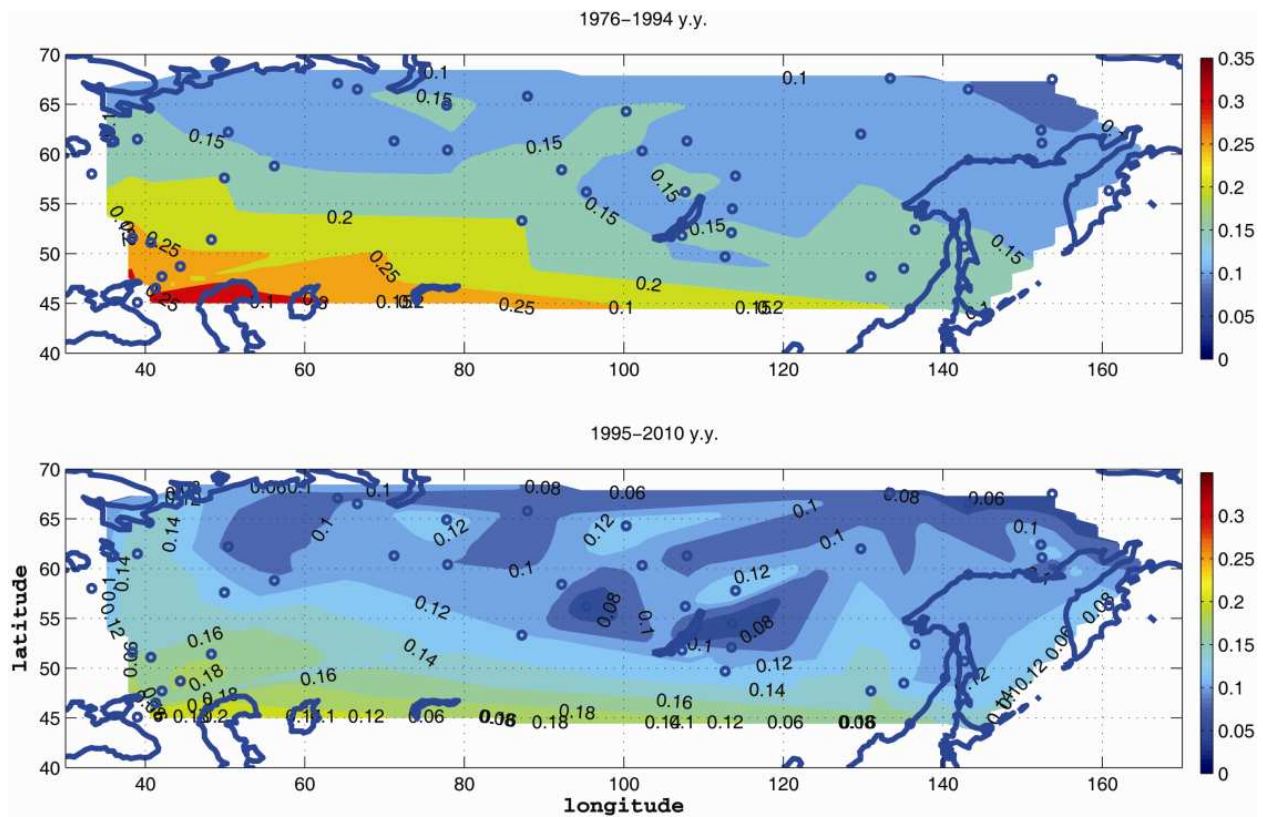


Figure 3. Spatial distributions of the multiyear means of AOD over the observation periods 1976–1994 (upper part) and 1995–2010 (lower part).

The annual values of AOD for each of the stations multiyear means over 1976–1994 years, over 1995–2010 years, their standard deviations are given in Fig.2. Each column of the diagram corresponds to the longitude position of the station in accordance with Table 1. The means of the AOD characteristics are corresponds to the multiyear (1976–1994 years) annual means of AOD (black), grey corresponds to the multiyear (1995–2010 years) annual means, red corresponds to standard deviations of the annual values of AOD from its mean for each station. A spatial distribution of AOD is shown in more detail in the maps (Fig. 3) drawn by interpolating the data obtained at 53 stations to Russia’s territory. For this interpolation, the technologies of the MATLAB 7.5.0. program package were used: there are options to create a uniform grid for the entire region, onto which the given functions $Z = F(x, y)$ were projected, where x and y are the latitude and longitude, respectively, for each of 53 observation points, and Z is the AOD mean. In addition, a bilinear interpolation of data was performed. Under bi-cubic and bi-square interpolations, the results, in principle, do not differ from those given in Fig. 3. The spatial distribution of the AOD means over the 35 - year period is in a good agreement with the results of modeling a spatial atmospheric-aerosol distribution, which are given in the IPCC third report (IPCC, Climate Change 2007). The model described in this report takes into account aerosols of different origins anthropogenic and natural sulfates, organic particles, soot, mineral aerosol of natural origin, and marine saline particles) which have certain specific properties of distribution over the globe, and it yields a decrease in AOD over Eurasia from the southern to the northern latitudes in the presence of areas with increased atmospheric turbidity over southern Europe, the Middle East, southeastern Asia,

Ukraine, and Kazakhstan. Fig. 3 shows that the AOD over Russia decreases from the southwest to the northeast. The increased values of aerosol haziness in the southeast and southwest are most likely caused by an advective arrival of air masses from the regions with high aerosol content in the atmosphere: from Ukraine and Kazakhstan in the southwest and from southeastern Asia and China in the southeast. Fig. 3 (upper part) shows the localizations of regional tropospheric aerosol sources (western and eastern Siberia and Primorskii Krai). In the last 15 years (Fig. 3, lower part), in the absence of powerful volcanic eruptions and under conditions the atmosphere being purified of the stratospheric aerosol layer, the sources of aerosol arriving in the troposphere have become more pronounced. In addition, in the last decade, the AOD has noticeably increased for a few stations in the Far East, which is probably due to increased volcanic activity on Kamchatka .

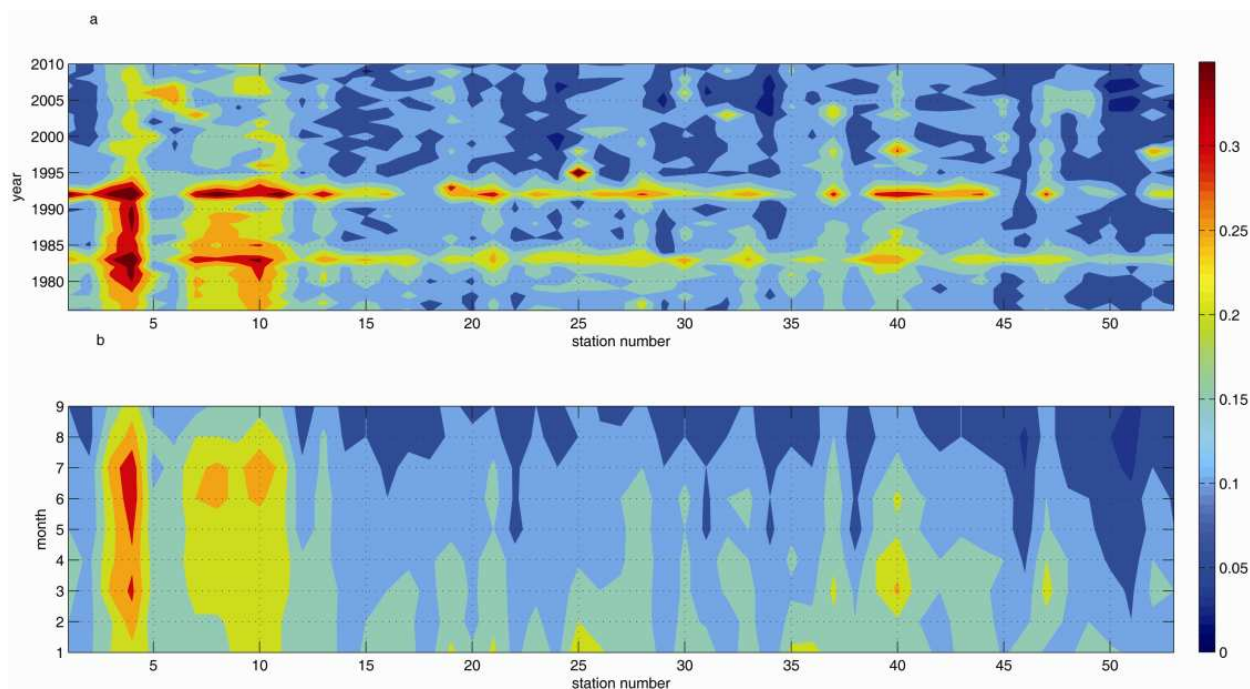


Figure 4. Spatiotemporal variations in AOD: (a) multiyear variations in the annual values of AOD for all 53 stations under consideration and (b) mean seasonal variations in AOD for all 53 stations under consideration.

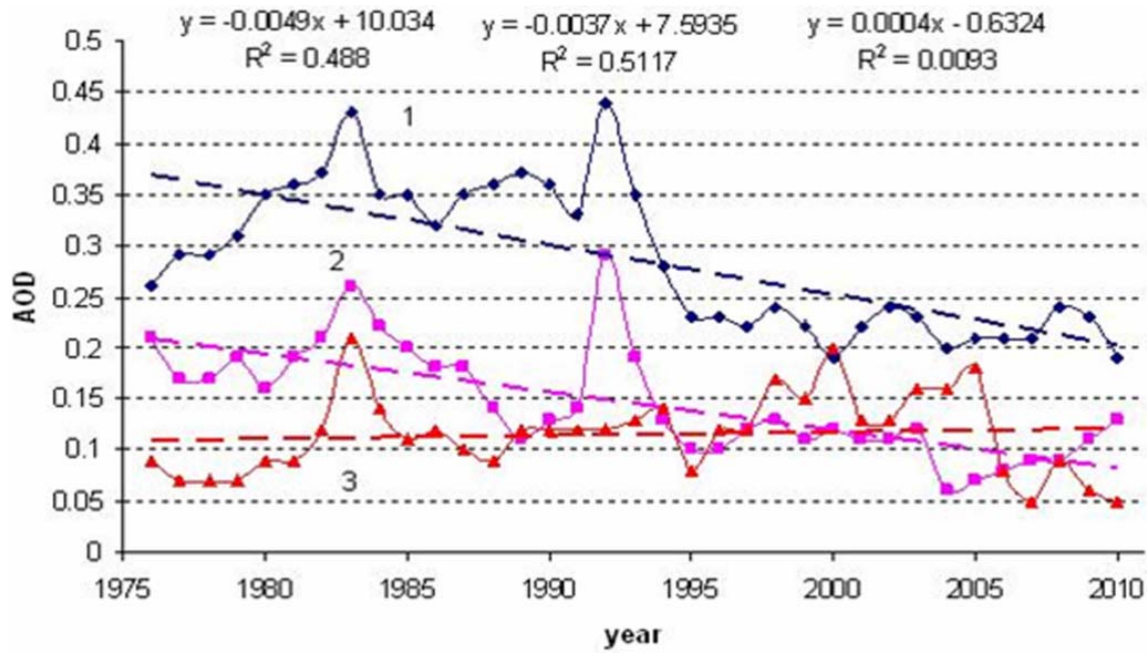
The spatiotemporal inhomogeneities of the AOD annual values clearly reflect their causes (Fig. 4a): the peaks of the volcanic eruptions (El Chichon, 1982, and Pinatubo, 1991) and the tundra fires of the last decade in eastern Siberia, the frequency and intensity of which have increased due to climate changes. Fig. 4b shows variations in the mean annual cycle of AOD. The features of the AOD mean annual cycle for each concrete station are formed under the influence of seasonal variations in the character of air-mass transport to a given point from regions with different aerosol contents (synoptic processes) and seasonal variations in air temperature, humidity, and in the state of the underlying surface, in combination with an industrial load of some regions. The AOD maxima are, as a rule, observed in April and July–August, but the summer maximum is more pronounced at stations (N° 4, 8, 9, 10, and 11) located in the south of European Russia. First of all, this is related to the fact that, in

summer, tropical air masses dominate here which are characterized by high contents of moisture and aerosol. The spring maximum is caused by snow cover melting and the replacement of the dominating arctic air masses by temperate or tropical air masses.

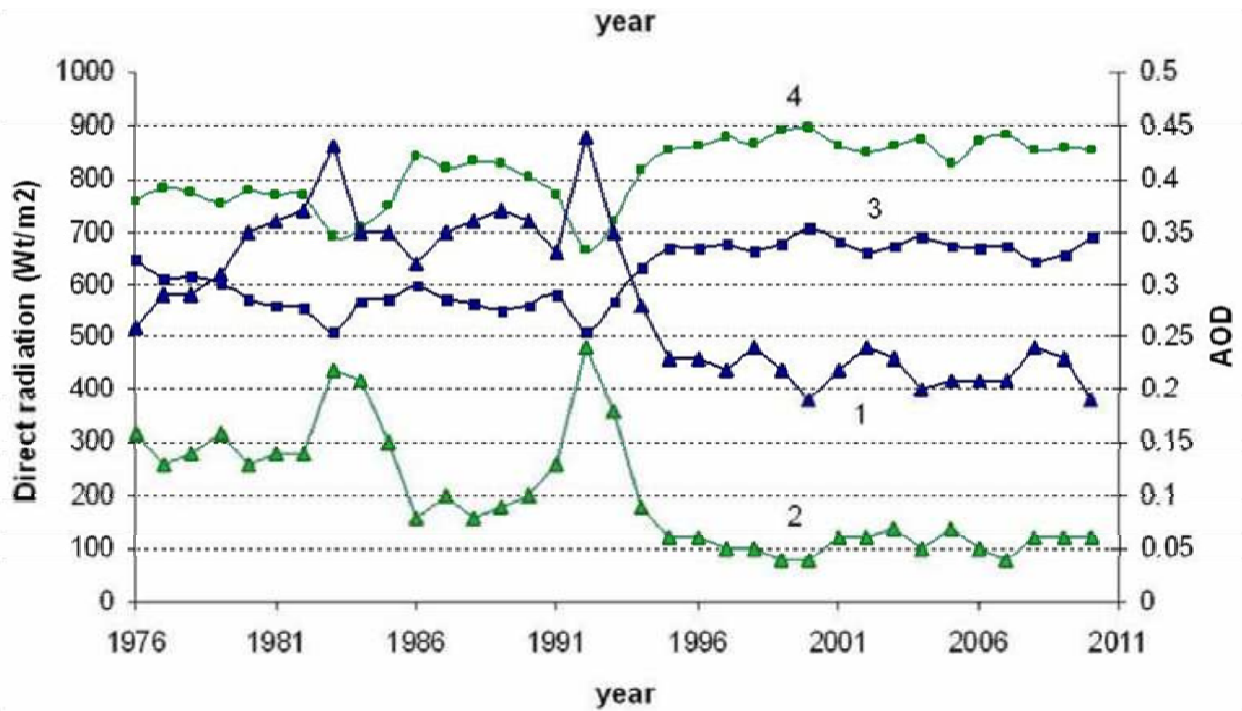
5. Time variations in aerosol optical depth AOD

Fig. 5a gives some examples of time variations in the annual means of AOD for stations with negative and positive trends. In Fig. 7b, the examples of the time trends of the AOD annual values are supplemented by the corresponding variations in the flux of direct solar radiation (for the Sun's height $h=30^\circ$), which reach 100 W/m^2 over the course of 35 years (3 W/m^2 per year); estimates were obtained for two stations with the maximum and minimum means of AOD. Thus, the influence of a decreased aerosol load on the flux of direct solar radiation incident upon the land surface under clear skies is empirically estimated. For total radiation, this influence is less pronounced. And our estimate of the rate of a decrease in direct solar radiation does not contradict the satellite data (IPCC, Climate Change 2007) on the rate of a decrease in the flux of the total reflected (upward) solar radiation ($-0.18 \pm 0.11 \text{ W/m}^2$ per year (the ISCCP project) and $(-0.13 \pm 0.08) \text{ W/m}^2$ per year (the ERBS project)) over the course of 1984–1999 and the assumption made in (IPCC, Climate Change 2007), that this is caused by a global decrease in stratospheric aerosol (the so-called phenomenon of “aerosol dimming”).

At most observation sites, the atmosphere was purified of aerosol within the period under consideration. On the whole, for Russia, the trend of AOD variations is negative (Fig. 6); the absolute value of the trend (over 10 years) varies from (-0.05) to $(+0.02)$ and increases generally from the south-west to the north-east of Russia. The mean of the relative trend accounts for (-14%) over 10 years, its maximum is 21% over 10 years, and its minimum is (-35%) over 10 years at a determination coefficient of no more than 0.5. (See also Table 1). It is evident that, in this case, a decrease in the AOD mean must be observed during the last 15 years of the whole region. The largest negative trends are observed at the Solyanka station (in the south of the Krasnoyarsk Krai), in Chita (Transbaikalia), Khabarovsk (Primorskii Krai), and in the south of European Russia. The combination of the two factors—global purification of the atmosphere from transformed volcanic aerosol and decreased anthropogenic forcing—forms the negative trends in these regions. Positive trends are observed in Arkhangelsk and the Far East (Kamchatka and Okhotsk), and almost zero trends are observed in western (station nos. 18, 19, and 20) Siberia. The positive (Arkhangelsk) and decreased negative (the indicated Siberian stations) trends may be caused by increased industrial emissions in these regions, an increase in the number and intensity of fires, and comparatively low-power volcanic eruptions (for example, in Kamchatka). The estimates of the AOD trends and integral transparency obtained by other authors (for example, Ohmura, 2006) were compared with our estimates earlier in (Plakhina et al., 2007). This comparison shows an agreement with the results presented in this paper.



(a)



(b)

Figure 5. Time variations in the annual values of AOD and in the flux of direct solar radiation for the Sun’s height 30°: (a) multiyear variations in the annual values of AOD for three stations (Krasnodar (1), Chita (2), and Okhotsk (3)) and (b) multiyear variations in the annual values of AOD and in the annual mean of direct solar radiation flux at the Sun’s height 30° for the two stations with the maximum and minimum means of AOD. For both graphs, the period under analysis is 1976– 2010. Krasnodar(1 corresponds to AOD and 3corresponds to direct radiation), Solyanka (2 corresponds to AOD and 4 corresponds to direct radiation)

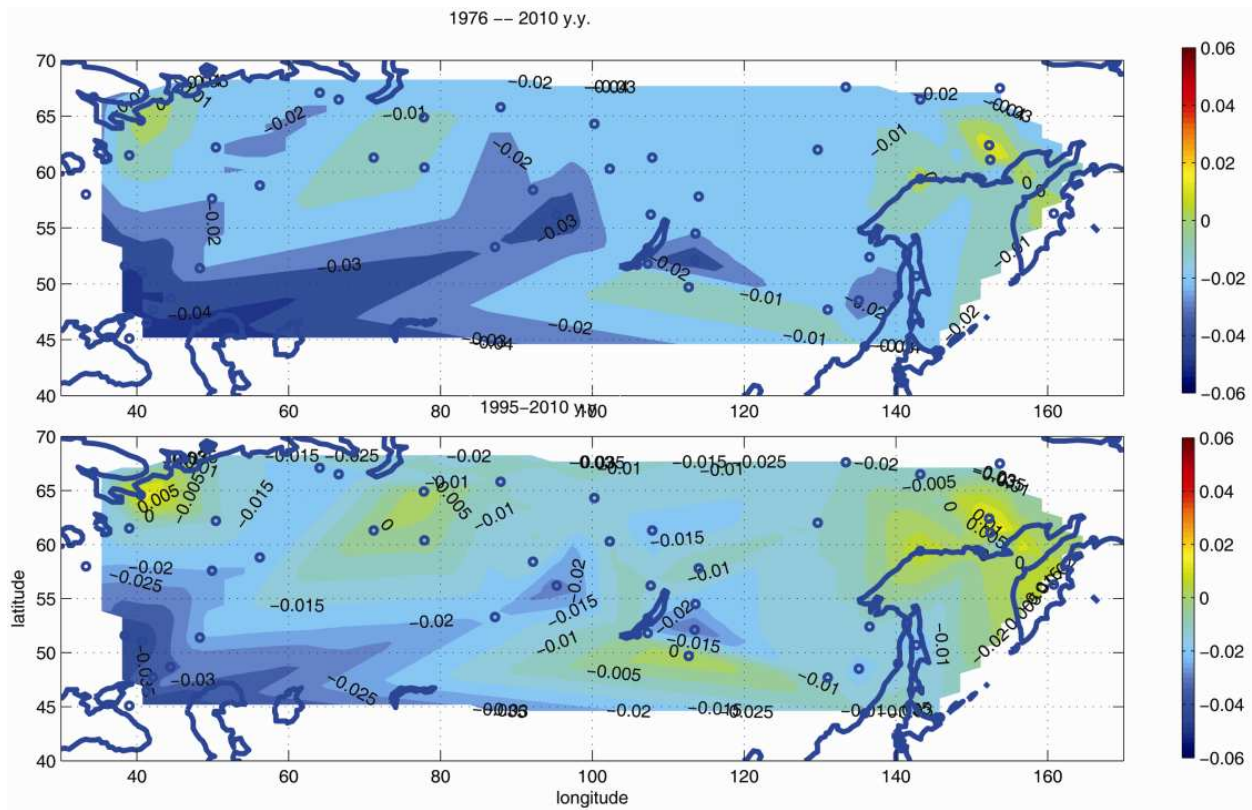


Figure 6. Spatial distributions of the multiyear variability of AOD: trends of the time variations over the period 1976–2010 years (in absolute values over 10 years) and trends of the time variations over the period 1995–2010 years (in absolute values over 10 years)

6. Effects of the volcano eruptions

6.1. Influence of the volcano eruption on AOD

Fig. 7 gives a “long” (45 years) series of annual means of AOD for the Ust’ Vym station (62.2°N, 50.4°E), which demonstrates a characteristic multiyear trend of variations in the annual values of AOD and its response to stratospheric disturbances. The four powerful volcanic episodes— Agung (8°S, 116°E, 1963), Fuego (14°N, 91°W, 1974), El Chichon (17°N, 93°W, 1982), and Pinatubo (15°N, 120°W, 1991)—are clearly pronounced and quantitatively estimated. In particular, the maximum effect observed a year after the eruptions is 100% (in deviations from the multiyear norm); throughout the year, its attenuation occurs with the dissipation and transformation of the stratospheric aerosol layer. A decrease in the AOD values for 1995–2006 is also clearly manifested. Such a character of multiyear variations in the annual values of AOD is characteristic of most stations and is, to a great extent, determined by the four powerful volcanic eruptions in the latter half of the 20th century, because seasonal and local disturbances caused by the effects of tropospheric aerosol, when annually averaged, become leveled and have almost no influence on the distribution of the multiyear values of AOD.

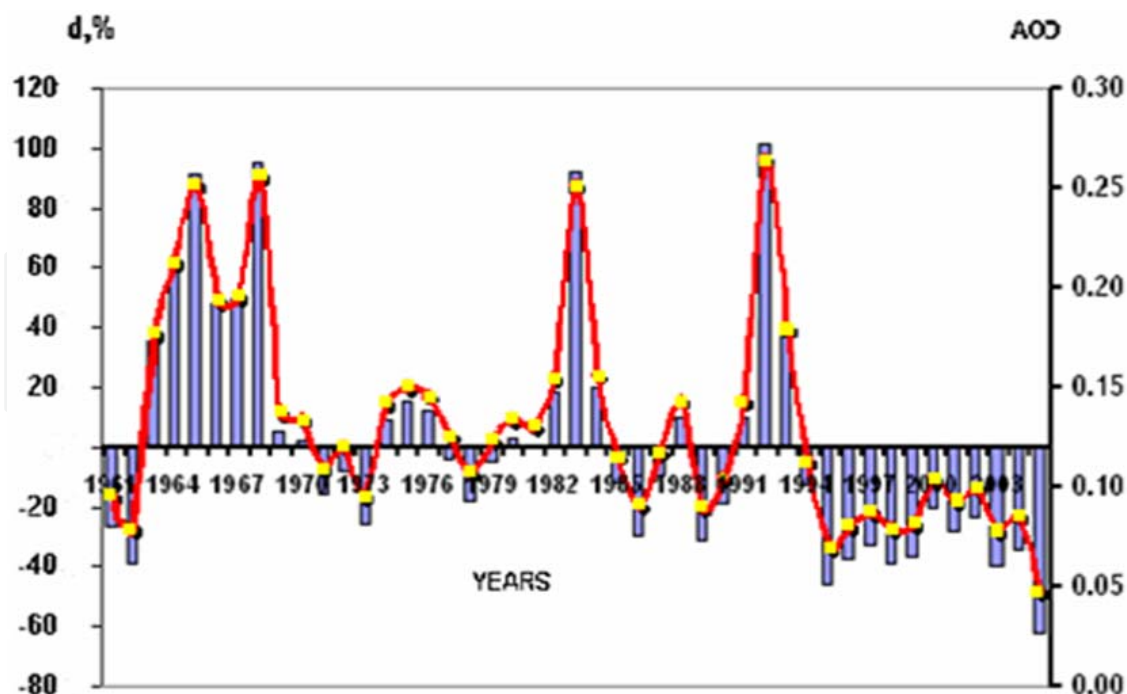


Figure 7. Example of multiyear variations in the annual means of AOD (red) and their deviations from the averaged (blue),

$$d = 100\% * (AOD_i - AOD_m) / AOD_m.$$

6.2. Influence of the volcano eruptions on the turbidity factor (T)

From the data of 80 observation stations over the Russia the special analysis of the turbidity factor (T) have been fulfilled: time variations during 1976-2010 y.y. and during 1994-2010 y.y. have been estimated. For the 9 regions over all Russia territory long-term trends for the characteristics of the integral atmospheric transparency have described. For all regions during 1976-2010 y.y. negative T and AOD variations tendencies exist; during 1994-2010 y.y. negative T and AOD variations tendencies remain at the same level as during 1994-2009 y.y. practically for all Russia regions. So, for the most part of Russia territory the conditions of the relatively high atmospheric transparency (in 1994-2010 y.y. – 17 years) remain as well as the atmospheric transparency increase within this 17 years time interval remain. Comparatively stable, longterm and intensive variations (increase) take place in post-volcanic periods: 1) for El Chichon eruption (1982 year, April) – from the last 1982 year to October of 1983 year; 2) for Pinatubo (1991 year, June) – from the September of 1991 year to July of 1993 year. Anomalies of the mean month values of the T₂ during these “post volcanic” period after the eruptions of El Chichon and Pinatubo are presented in Table 2.

Estimations of the volcano contribution into the multiyear mean values (for the months and year) of the factor turbidity and aerosol optical depth during 1976 – 2005 years period and during the so called “stable” 1976-2005 years period (without 1982, 1983, 1991, 1992, 1993 years) are pointed in Table 3. It is obvious that effects, connected with eruptions lead to increase of the multiyear mean values equal 3% (from 1% - to 7%) for T and equal 7% (from 2% - to 12%) for AOD.

Region	$\Delta T_2\% = 100 \cdot (T_i - T_m) / T_m$		$\Delta T_2 = (T_i - T_m) / \sigma$	
	El Chichon	Pinatubo	El Chichon	Pinatubo
North of EPR	20	32	1.9	3.0
Central part of EPR	18	30	1.8	3.1
South of EPR	14	20	1.8	2.6
Ural	26	23	2.6	2.3
West Siberia	19	35	1.7	3.1
North-east of APR	19	35	1.7	3.2
Central part of APR	19	27	2.0	2.8
South of EPR	22	38	1.8	3.0
Far East of the Russia	15	36	1.5	3.4

Table 2. Anomalies of the mean month values of the T during post volcanic period after the eruptions of El Chichon and Pinatubo.

Month	$T_{(1976-2005)} / T_{stab.(1976-2005)}$												Year
	1	2	3	4	5	6	7	8	9	10	11	12	
North of EPR		1,03	1,03	1,04	1,03	1,03	1,02	1,02	1,03	1,02	1,04		1,03
Central part of EPR	1,04	1,05	1,04	1,04	1,03	1,02	1,02	1,02	1,01	1,02	1,02	1,05	1,03
South of EPR	1,04	1,04	1,03	1,03	1,02	1,02	1,01	1,01	1,01	1,01	1,03	1,04	1,02
Ural	1,05	1,06	1,06	1,04	1,03	1,03	1,02	1,02	1,03	1,02	1,05	1,05	1,04
West Siberia	1,03	1,05	1,04	1,03	1,04	1,03	1,02	1,03	1,04	1,03	1,02	1,02	1,03
North-east of APR	1,07	1,07	1,04	1,03	1,03	1,03	1,03	1,02	1,02	1,03	1,05	1,07	1,04
Central part of APR	1,04	1,02	1,02	1,02	1,02	0,98	0,98	1,02	1,01	1,00	1,06	1,04	1,02
South of EPR	1,06	1,04	1,04	1,04	1,03	1,02	1,02	1,02	1,02	1,02	1,03	1,03	1,03
Far East of the Russia	1,06	1,05	1,04	1,03	1,02	1,02	1,01	1,01	1,01	1,02	1,03	1,05	1,03

Month	$AOD_{(1976-2005)} / AOD_{stab.(1976-2005)}$												Year
	1	2	3	4	5	6	7	8	9	10	11	12	
North of EPR		1,11	1,10	1,10	1,08	1,07	1,07	1,06	1,06	1,06	1,14		1,07
Central part of EPR	1,06	1,07	1,08	1,09	1,10	1,08	1,08	1,07	1,06	1,02	1,09	1,10	1,07
South of EPR	1,10	1,09	1,06	1,07	1,05	1,04	1,03	1,02	1,03	1,04	1,10	1,14	1,06
Ural	1,08	1,12	1,14	1,11	1,09	1,08	1,07	1,08	1,14	1,08	1,07	1,08	1,06
West Siberia	1,05	1,10	1,11	1,09	1,11	1,10	1,08	1,06	1,08	1,13	1,07	1,08	1,08
North-east of APR	1,03	1,13	1,11	1,08	1,09	1,08	1,08	1,07	1,09	1,11	1,13	1,02	1,09
Central part of APR	1,08	1,07	1,08	1,09	1,10	1,08	1,08	1,07	1,06	1,05	1,13	1,11	1,06
South of EPR	1,09	1,08	1,09	1,10	1,08	1,05	1,05	1,05	1,05	1,04	1,06	1,06	1,07
Far East of the Russia	1,12	1,11	1,09	1,06	1,06	1,07	1,06	1,03	1,04	1,04	1,08	1,12	1,07

Table 3. Estimation of the volcano contribution into the multiyear mean values of the factor turbidity and aerosol optical depth during 1976 - 2005 years period; EPR -- the European Part of Russia; APR -- the Asian Part of Russia.

The examples of the long-term time variations for T and AOD in the different Russia regions: North, Central part and South of the European Part of the Russia and Russian Far East are presented in Fig. 8.

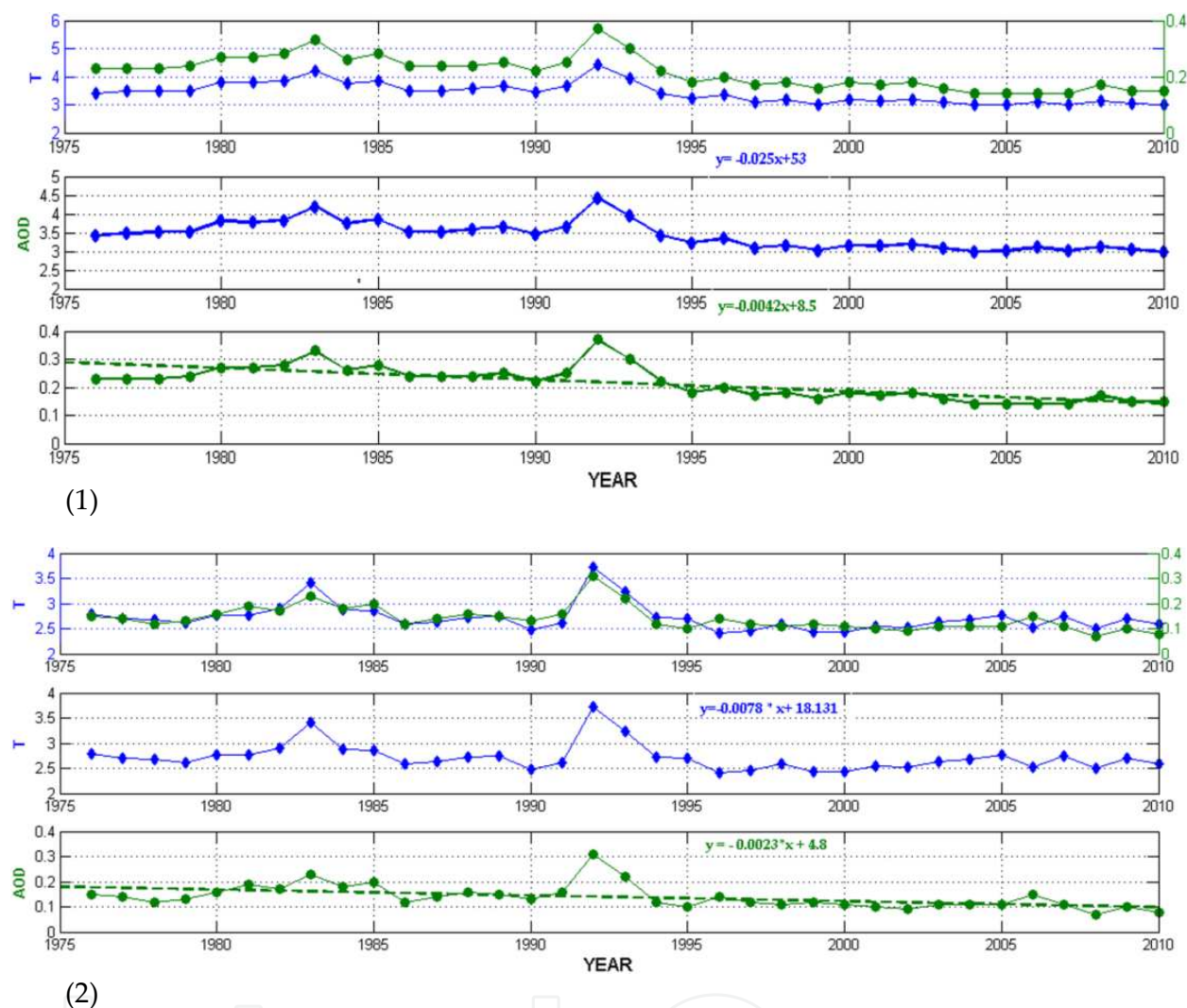


Figure 8. Examples of the long-term time variations for T (blue) and AOD (green) in the different Russia regions: South of the European Part of the Russia (1) and North part (2).

7. Fires above the European Part of Russia (EPR) under conditions of abnormal summer of 2010

The spatial variations in the air turbidity factor according to ground-based measurement data from 18 solar radiometry stations within the territory (40° – 70° N, 30° – 60° E) in summer 2010. We have shown earlier (Makhotkina et al., 2005; Plakhina et al., 2007, 2009, 2010) that the spatial distribution of the aerosol optical depth (AOD) over the territory of Russia averaged over more than 30 years corresponds to the model of global atmospheric aerosol distribution over Eurasia and the satellite AOD monitoring results, presented in the 3rd and 4th IPCC reports; it shows a decrease in the aerosol turbidity from southwest to northeast.

The events of summer 2010 (abnormal heat and forest and peat fires) evidently changed both the average values of air turbidity and the character of its spatial variations. Therefore, our estimates are of interest in the analysis (All Russia Meeting, 2010) of the situation on the European Part of Russia (EPR) in summer 2010. Fig. 9 presents the coordinates of solar radiometry stations on the EPR (Luts'ko et al., 2001); data from it were used in this work. The long-term annual average (over a “post-volcanic” period of 1994–2009 years) values T_{post} for summer months and the corresponding monthly values T_{2010} for 2010 are given in Table 4, along with the monthly average maxima of T and the relative difference (%) $D = (T_{2010} - T_{\text{post}})/T_{\text{post}}$. As it is seen, the average July and August T in 2010 and in the “postvolcanic” period differ by -6% and $+4\%$, respectively (the differences D vary from -28% to $+11\%$ of the average value for a certain station in June and from -22% to $+25\%$ in July). The value of $D = (T_{2010} - T_{\text{post}})/T_{\text{post}}$ is 14% in August (for the region) and varies from -11% to $+48\%$ for certain stations.

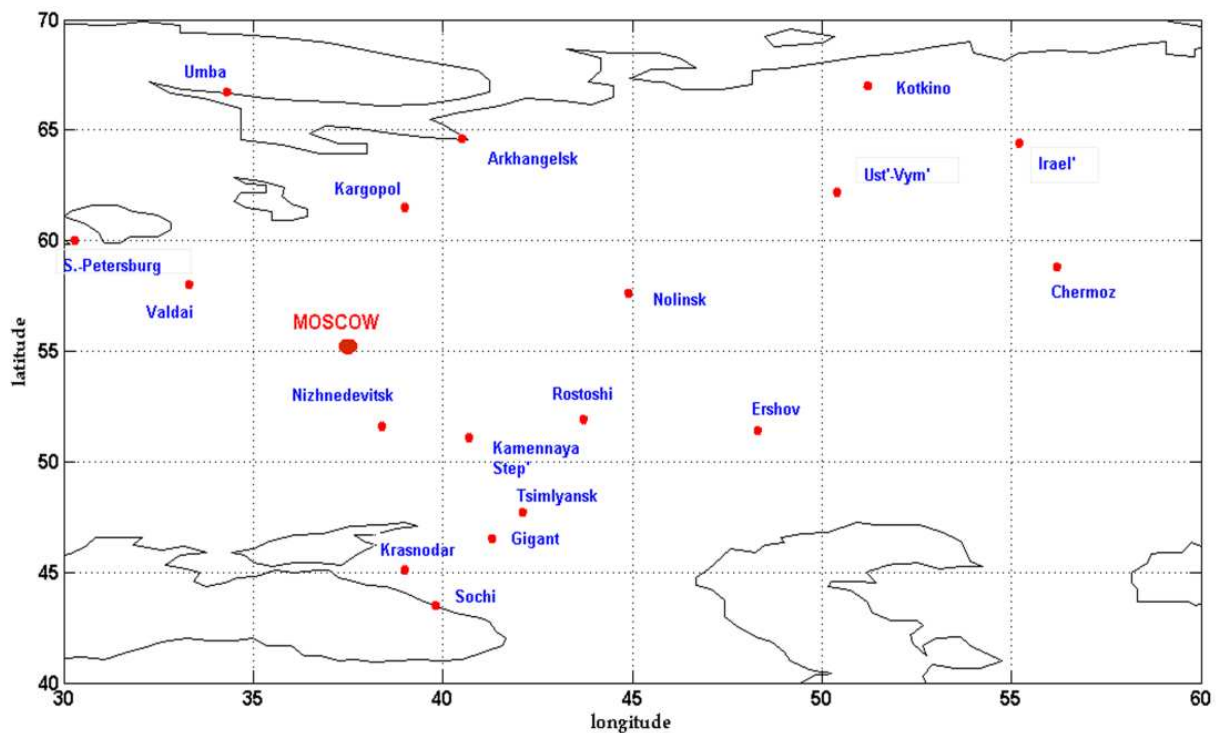


Figure 9. Layout of 18 actinometric stations on the EPR whose data will be analyzed in this section.

Spatial variations in T_{are} are shown in Fig. 10. To interpolate the data of the stations to the whole region under study, we also used features of the MATLAB package, i.e., the option for creating a homogeneous grid for the EPR region under study, the option of bilinear (horizontal and vertical) interpolation of data from 18 stations to the territory (40° – 70° N, 30° – 60° E), and the projection of the function $T = F(\phi, \lambda)$ (where ϕ and λ are the longitude and latitude, respectively, for each of the observational points) to the grid. The spatial distribution of the mean T_{post} (for June, July, and August) for the “postvolcanic” period corresponds to the results obtained earlier (Plakhina et al., 2009) for the long-term annual average AOD. In this period, T_{post} quasi-monotonically decreased from southwest to

Period	Month	Mean (maximum)	D	Standard deviation in the series of monthly average values for different stations
1994 – 2009 years	June	3.0 (3.9)		13%
	July	3.2 (4.2)		13%
	August	3.2 (4.3)		14%
2010 year	June (165)	2.95 (4)	-6%	18%
	July (250)	3.42 (4.1)	+4%	19%
	August (125)	3.73 (5.3)	14%	21%

Table 4. Long-term monthly average values of the turbidity factor T (1994-2009 years) and the corresponding values for summer 2010 along with the regional maximum values of mean T . The number of daily average values of T used in the averaging is mentioned in the parenthesis in the second column.

northeast; the regions of localization of regional tropospheric aerosol sources are invisible (except for Archangelsk). The June–July average values of T at the Archangelsk station have been increased during the “postvolcanic” period: a local (and/or regional) atmospheric aerosol source is traceable; it can be both frequent natural forest fires and anthropogenic industrial factors in this Russian region. The pattern differed significantly before 2010. In June, the spatial variations in T were close to distributions of T_{post} with a certain northward shift of the regions of maximum transparency ($T = 2 - 2.5$) with a decrease in means for June (Table 2) throughout the region in comparison with the “postvolcanic” period. In July, the monotonicity in a decrease in the turbidity was obviously disturbed in the northeast direction. A south-to-north “tongue” of increased values of the turbidity factor is observed ($T = 3.5 - 4.0$). Finally, in August, an epicenter (closed region) of anomalous air turbidity ($T = 4.5 - 5.5$) was formed within the region $48^\circ - 55^\circ \text{ N}$ and $37^\circ - 42^\circ \text{ E}$, which is located to the south of Moscow and covering the Moscow region by its periphery ($T = 4.0 - 4.5$). This pattern resulted from the action of the blocking anticyclone, which prevented air mass ingress from the west, provided for closed air circulation in the EPR, and a favored temperature rise over the EPR and a rapid increase in the forest fire area. Fire aerosols accumulated in the atmosphere through this period. This process was the most pronounced in the 1st decade of August. Our pattern of spatial distribution of T in August 2010, obtained from ground based measurements of the direct solar radiation flux, is in a good agreement with the map of AOD distribution in the EPR (within the region $50^\circ - 65^\circ \text{ N}$, $30^\circ - 55^\circ \text{ E}$) in the 1st decade of August presented in (Sitnov, 2010).

Thus, we have ascertained the peculiarities of spatial variations in the air turbidity factor in summer 2010 in comparison with the long-term average spatial variations, which have been manifested in both distribution character and the value of the anomalies of the turbidity factor.

8. Changes in integral and aerosol atmospheric turbidity in Trans-Baikal and Central Siberia

The turbidity factor T and atmospheric aerosol optical thickness AOD for the wavelength 0.55μ is used in this section as atmospheric transparency characteristics. The series T and AOT were analyzed for the 1976–2010 years for the stations presented in Fig.11.

From Fig. 12, 13 and Table 5 it is evident that AOD and T have the apparent seasonal dependence: maximal values of the aerosol turbidity are observed in spring (mean excess above the year ones is 25%), maximal values of the integral turbidity are observed in summer (mean excess above the year ones is 10%). At the same time the structure of the spatial distribution is similar in April and in July as for AOD so for T . The sources, formed AOD and T spatial distribution: prevailing air circulations, bearing of the aerosol and water vapor rich air masses (and vice versa), “constant” local aerosol sources, antropogenic or natural (for example, the forest or peat fires).

From Fig. 14, 15 it is evident that in July it is exist the constant district in Trans-Baikal region with high AOD (may be the fires); in April a structure of the AOD field is formed by the air masses arriving from the south directions. But in April a structure of the T is not so apparent. In Fig.16 the variation of the month averaged values of FQ - fires quantity (aircraft data) and factor of integral turbidity T are showed. It is observed that FQ have seasonal variations with the maximum value in May, at the same time maximum for T is observed in July. We can also see the growth of T , connected with the El Chichon eruption in 1982 - 1983 years. In Fig.17 the wavelet spectra of the fire quantity (FQ) and factor of integral turbidity (T) series demonstrate the oscillations by 12 moths period (in both series) up to 1982-83 years (1982 y. - volcano eruption). Then the oscillations by 6 - 3 month periods are exist in the FQ series, which are connected with the variations of the FQ - fire quantity. Colorbar represents normalized variances.

In Fig.18 the variation of the month averaged values of fires quantity FQ (aircraft data) and factor of integral turbidity T are showed during 1992 -2009 years. It is also observed that the FQ have seasonal variations with the maximum value in May, at the same time maximum for T is observed in July. We can also see the decrease of T , connected with the Pinatubo eruption during 1992-1993 years. In Fig.19 the wavelet spectra of the fire quantity (FQ) and factor of integral turbidity (T) series demonstrate the oscillations by 12 moths period (in both series) from 1997 year up to 2005 year (in FQ series) and up to 2006 year (in T series) . Then the oscillations by 7- 3 monhs are exist in the FQ series, which may be also connected with the variations of the fire quantity. Colorbar represents normalized variances.

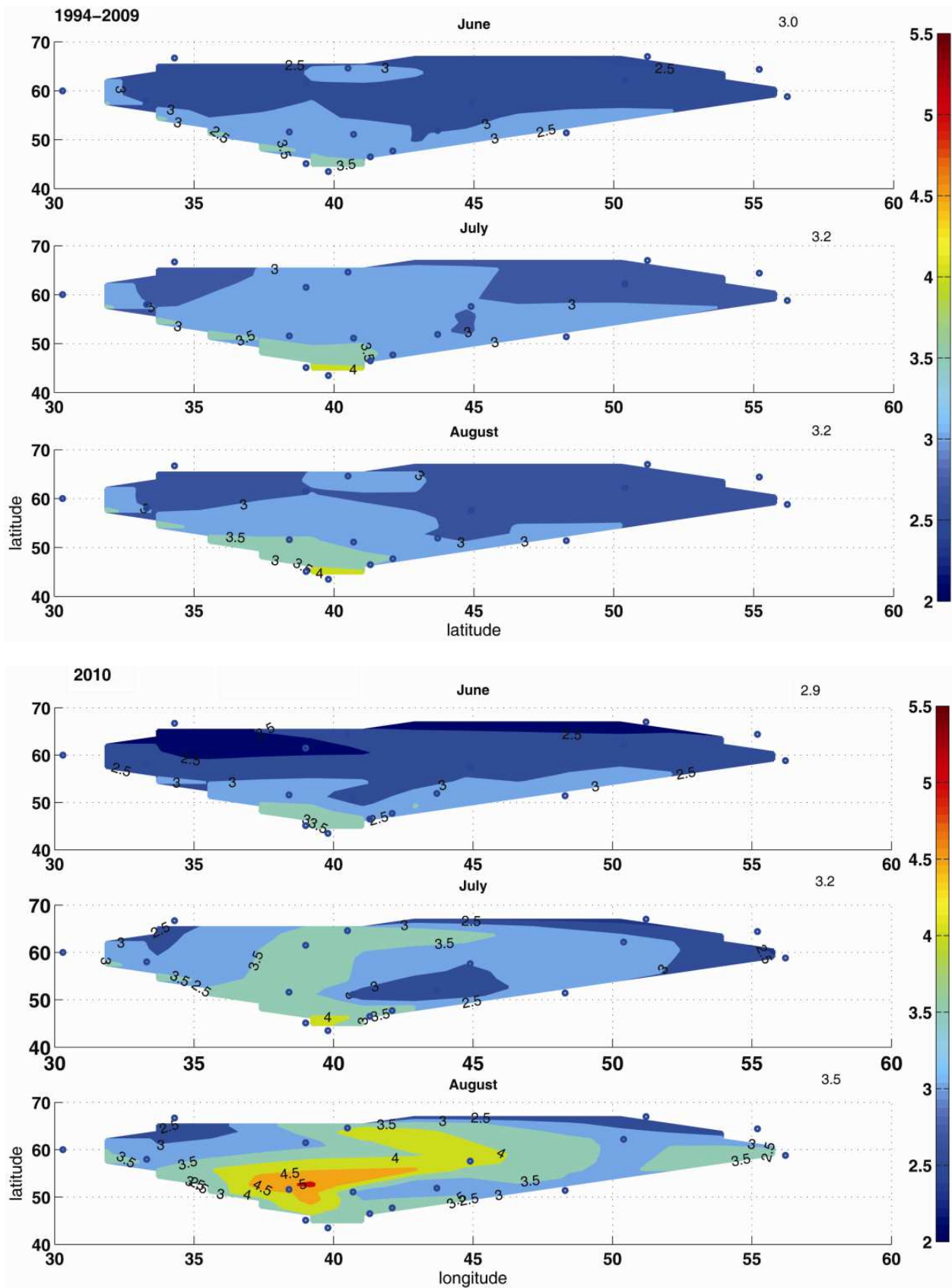


Figure 10. Spatial distribution of mean values of the turbidity factor T for June, July, and August in 1994 – 2009 years (top part) and in summer 2010 year (lower part).

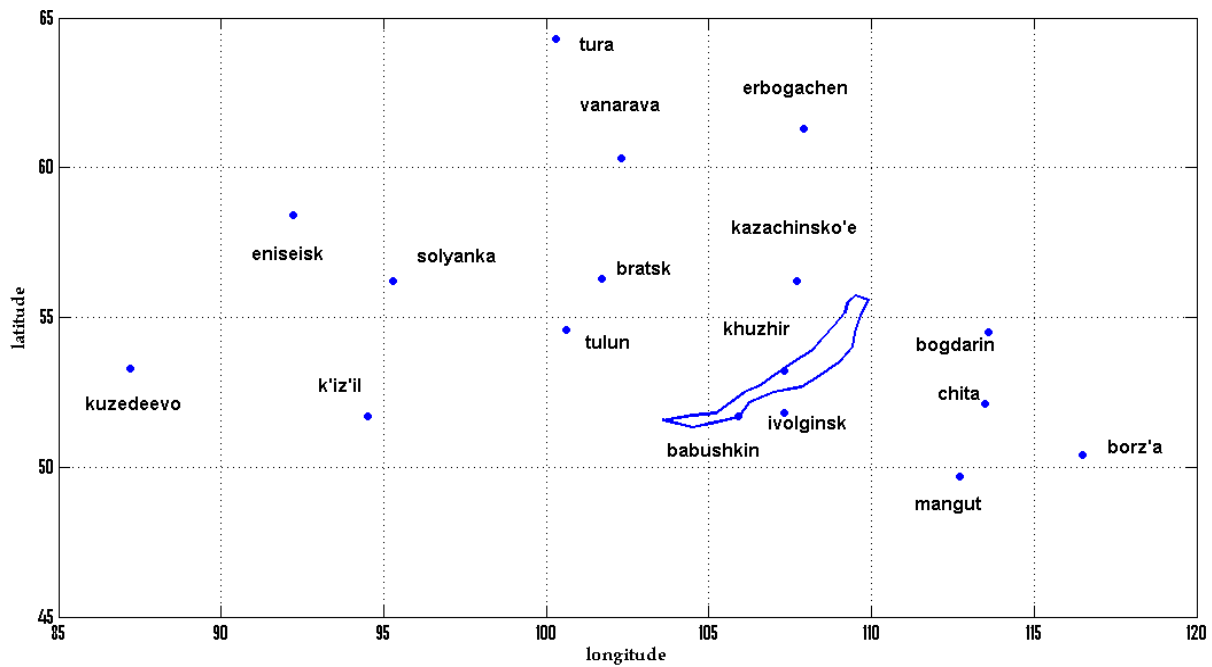


Figure 11. Layout of 17 actinometric stations whose data were analyzed in this section to investigate integral and aerosol atmospheric turbidity variability in Trans-Baikal and Central Siberia.

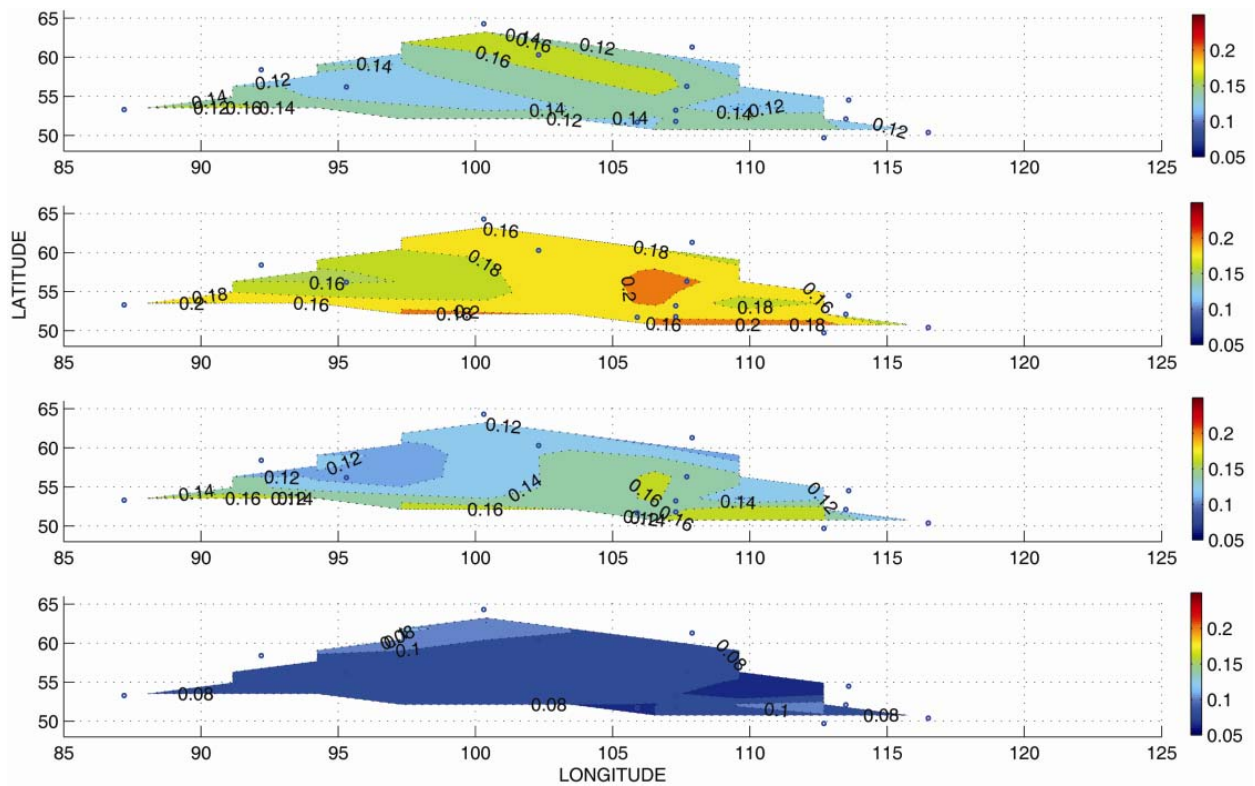


Figure 12. Spatial distribution of AOD in Trans-Baikal and Central Siberia region of Russia for the year and season AOD values: year, April, July and October values (from the top to the bottom), averaging period 1976-2010 years (14 stations).

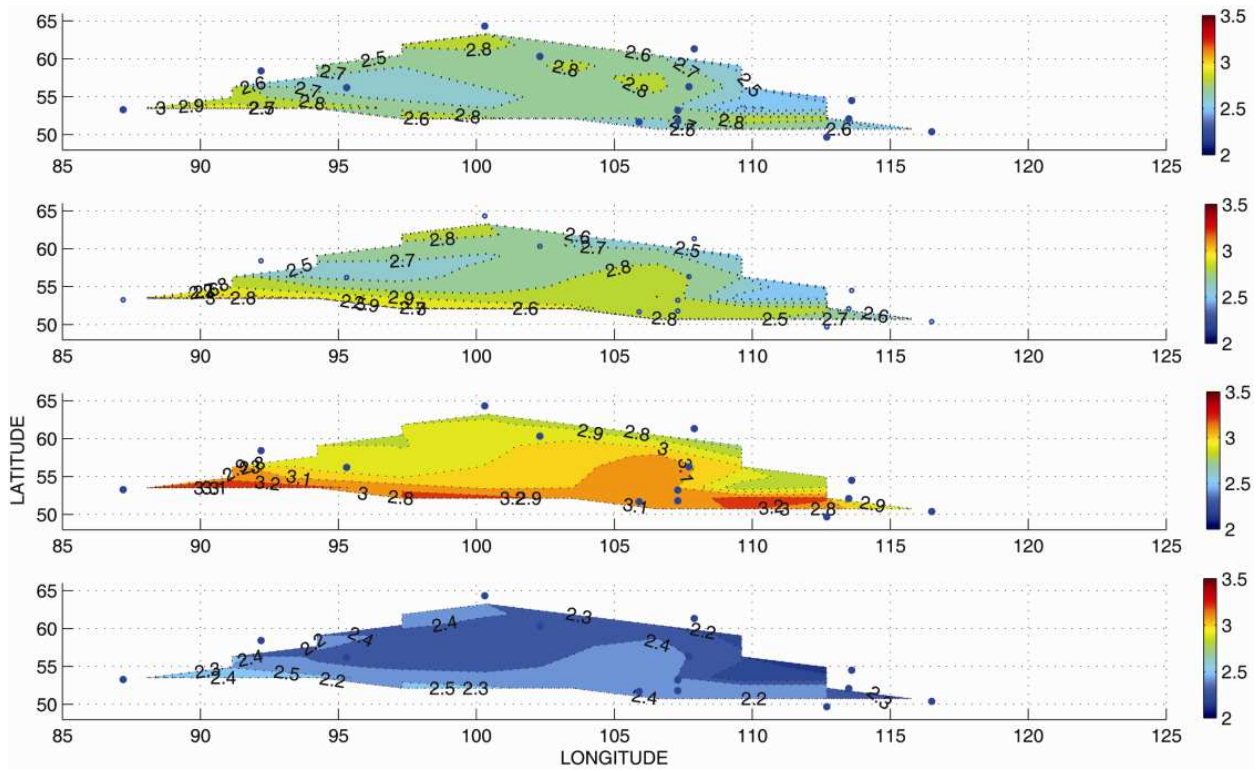


Figure 13. Spatial distribution of T in Trans-Baikal and Central Siberia region of Russia for the year and season AOD values: year, April, July and October values (from the top to the bottom), averaging period 1976-2010 years (14 stations).

	YEAR	APRIL	JULY	OCTOBER
AOD	0.14	0.19	0.14	0.09
variation coefficient %	13	16	15	16
turbidity factor T	2.72	2.76	3.02	2.39
variation coefficient %	36	43	44	66

Table 5. Multiyear mean values of the T turbidity factors of the atmospheric aerosol optical thickness (AOD) and their variation coefficients (the period of averaging is 1976–2010)

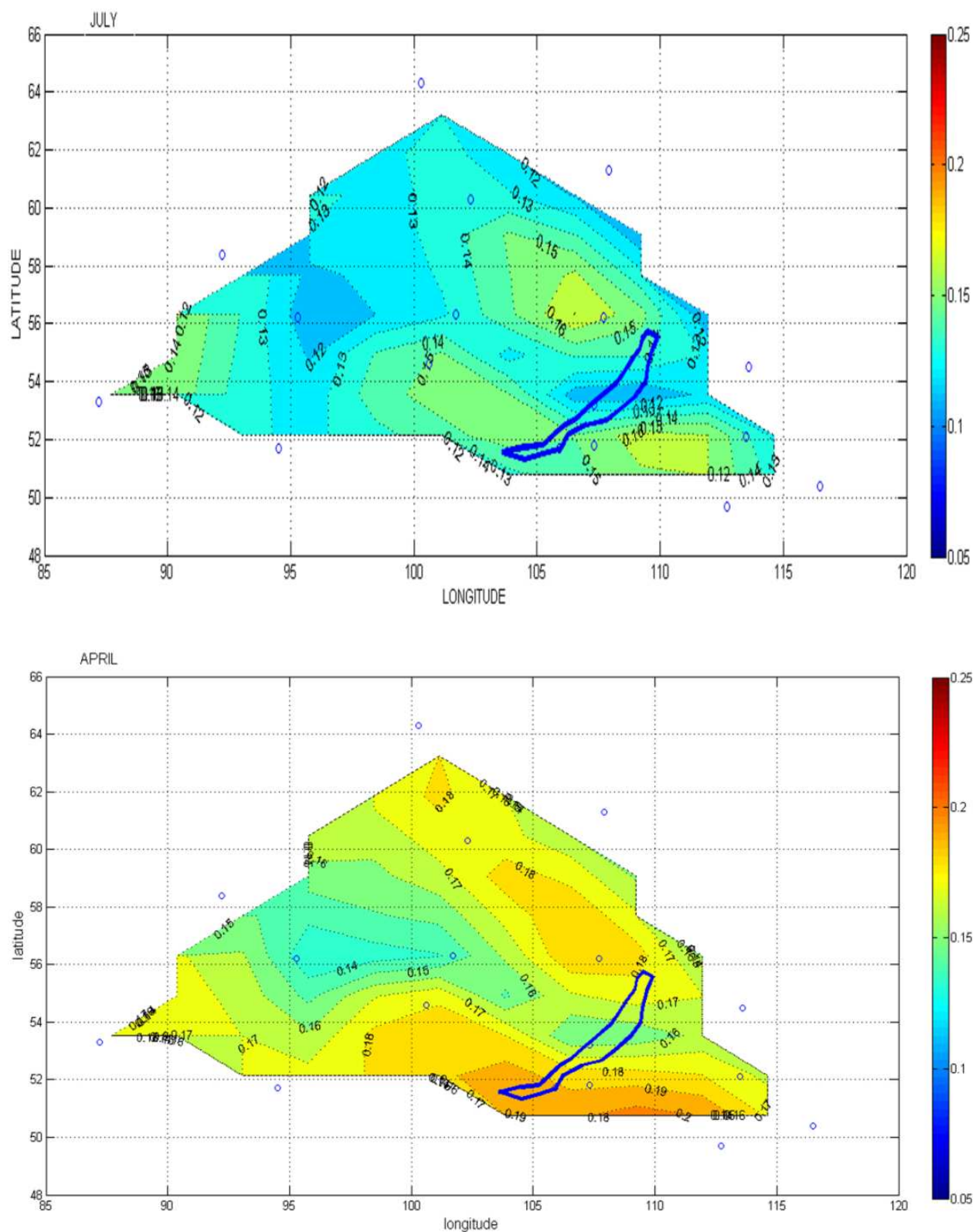


Figure 14. Spatial distribution of AOD in Trans-Baikal and Central Siberia region of RF for the July (top) and April (bottom) values, averaging period 1976-2010 years, 17 stations.

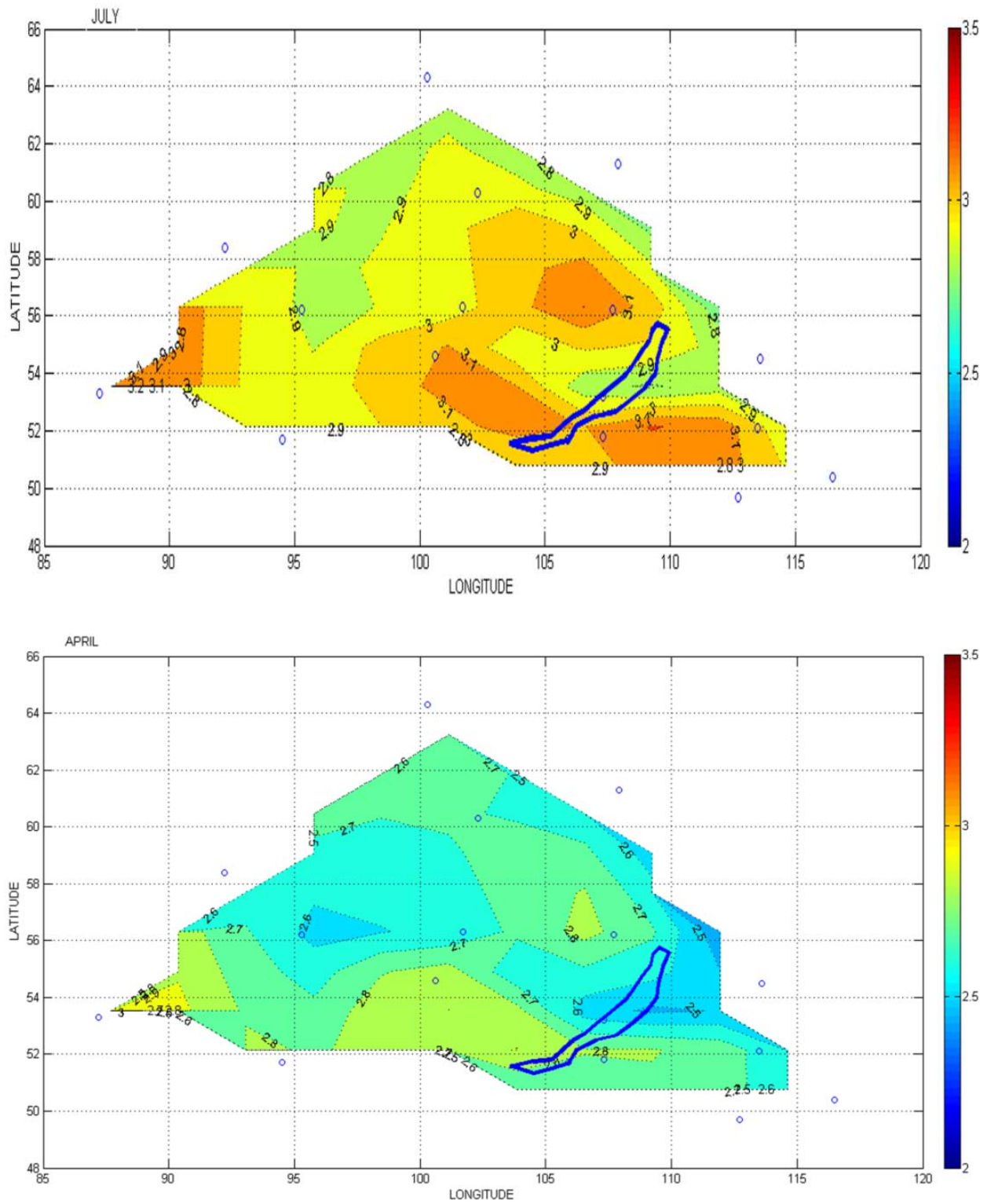


Figure 15. Spatial distribution of T in Trans-Baikal and Central Siberia region of RF for the July (top) and April (bottom) values, averaging period 1976-2010 years, 17 stations.

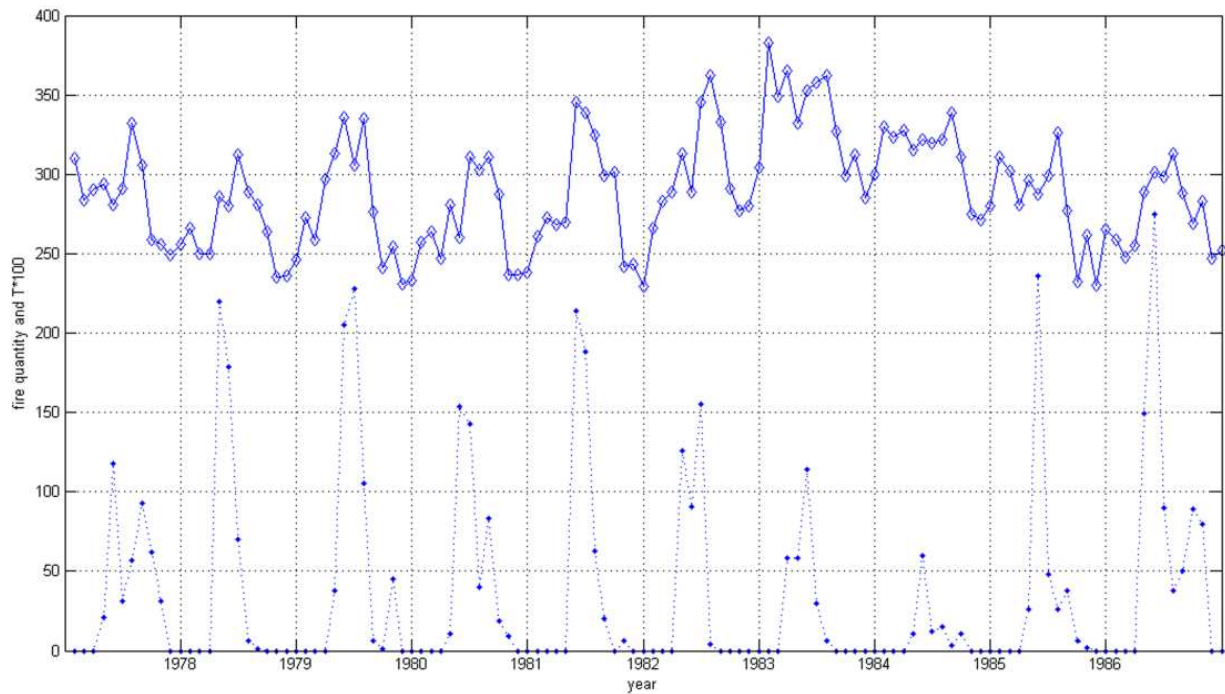


Figure 16. Fire quantity (FQ) (dotted line) and factor of integral turbidity T (firm line) during 1977 - 1986 years in Trans-Baikal region.

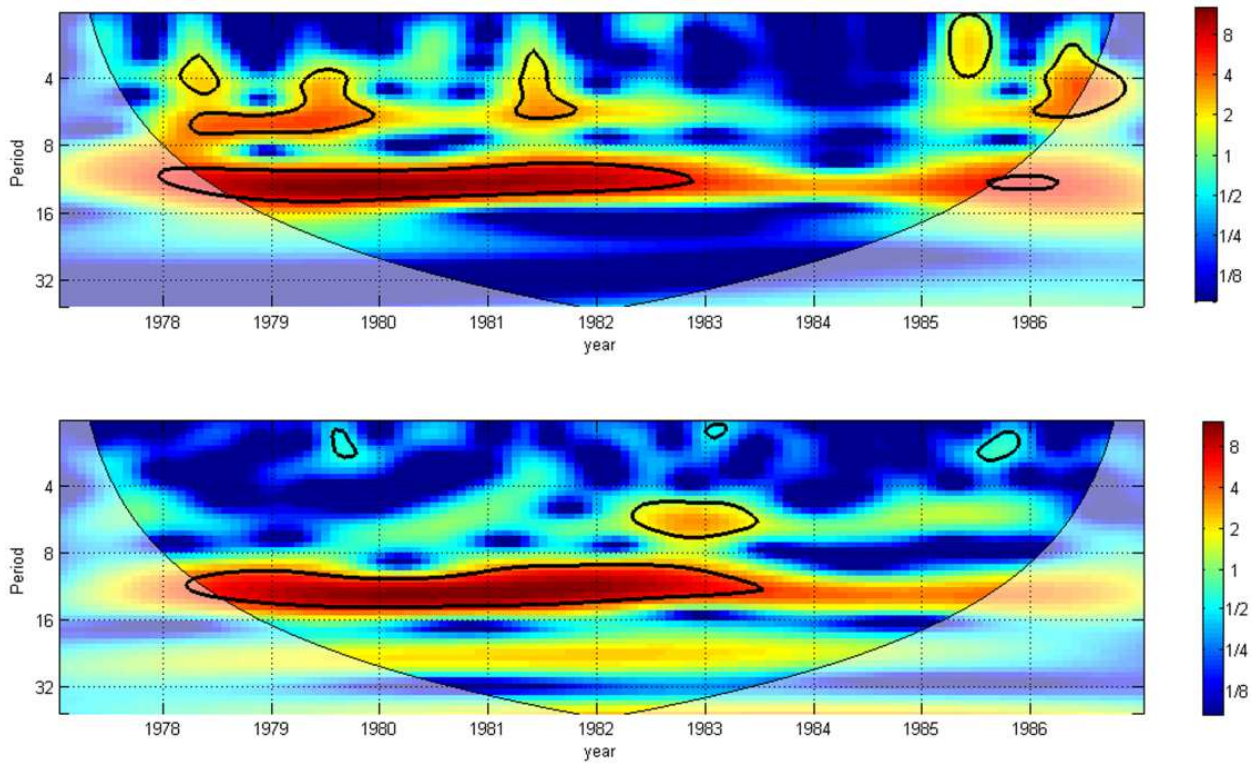


Figure 17. A result of the one-dimensional wavelet transformation of the two signals: fire quantity FQ (top) and factor of integral turbidity T (bottom) during 1977 -1986 years in Trans-Baikal region.

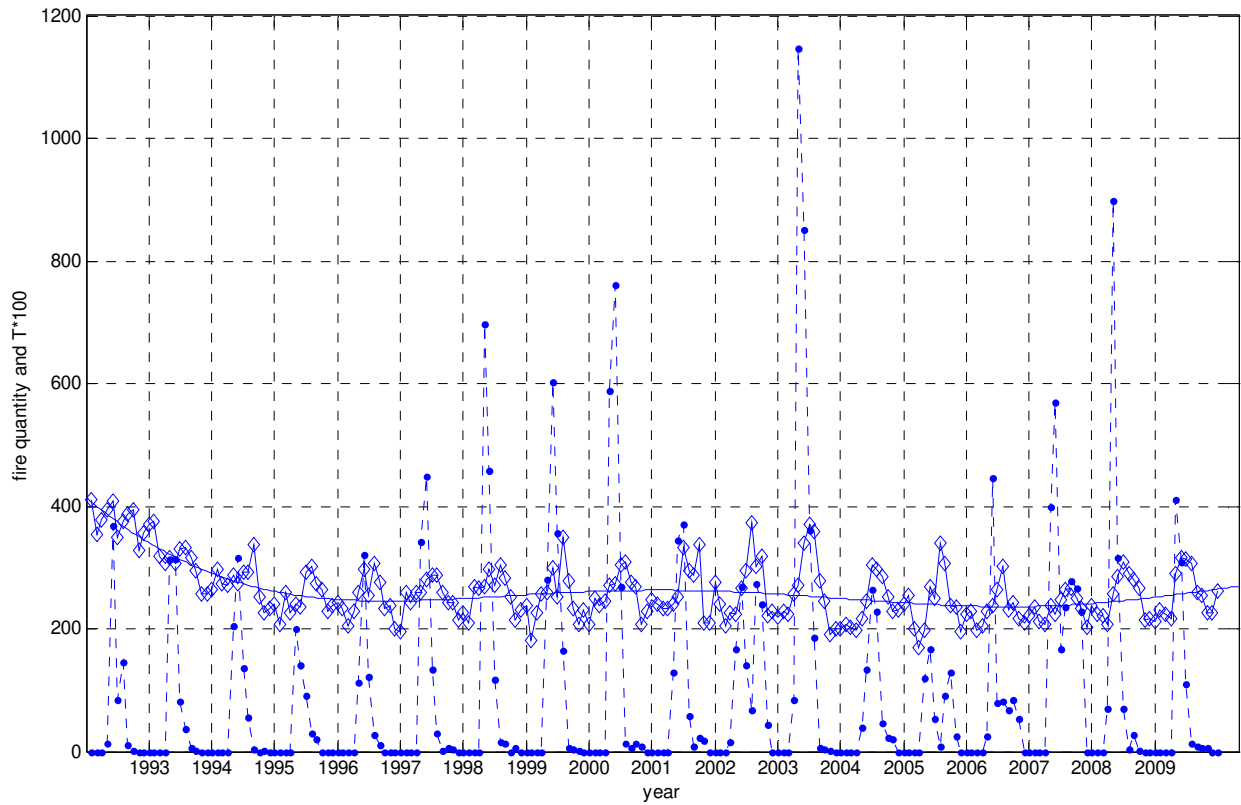


Figure 18. Fire quantity FQ (dotted line) and factor of integral turbidity T (firm line) during 1992 - 2009 years in Trans-Baikal region.

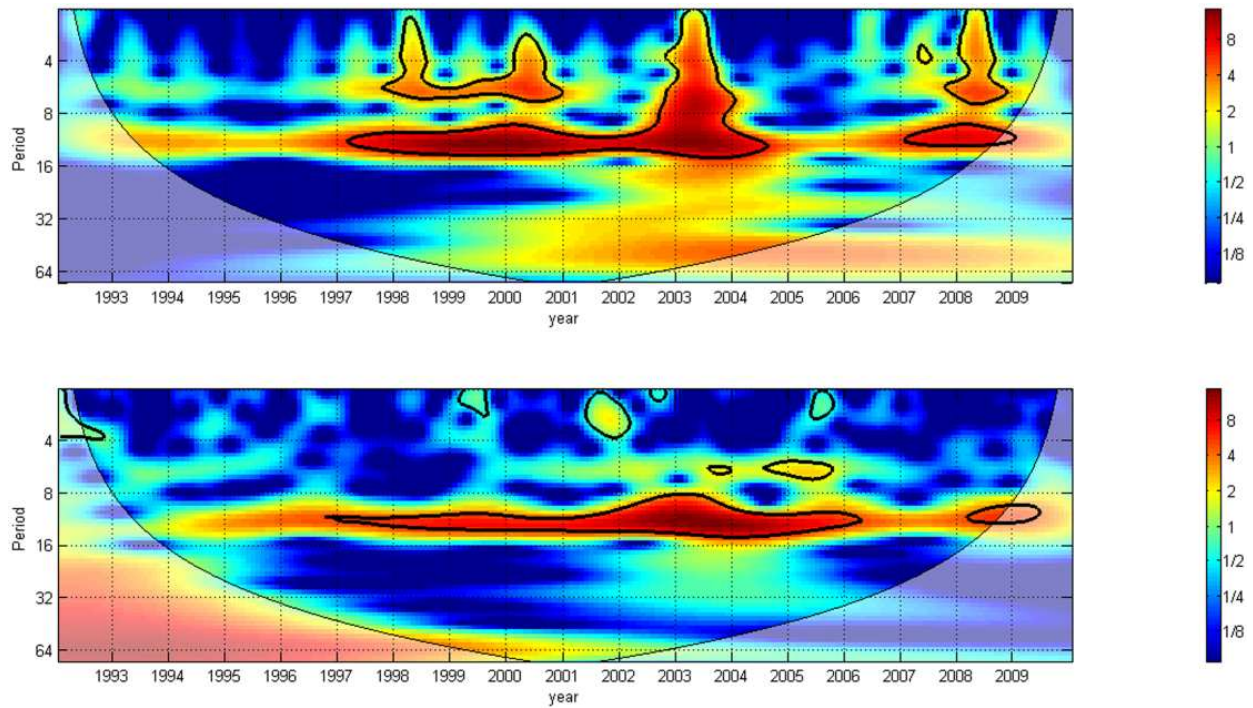


Figure 19. A result of the one-dimensional wavelet transformation of the two signals: fire quantity FQ (top) and factor of integral turbidity T (bottom) during 1992 - 2009 years in Trans-Baikal region.

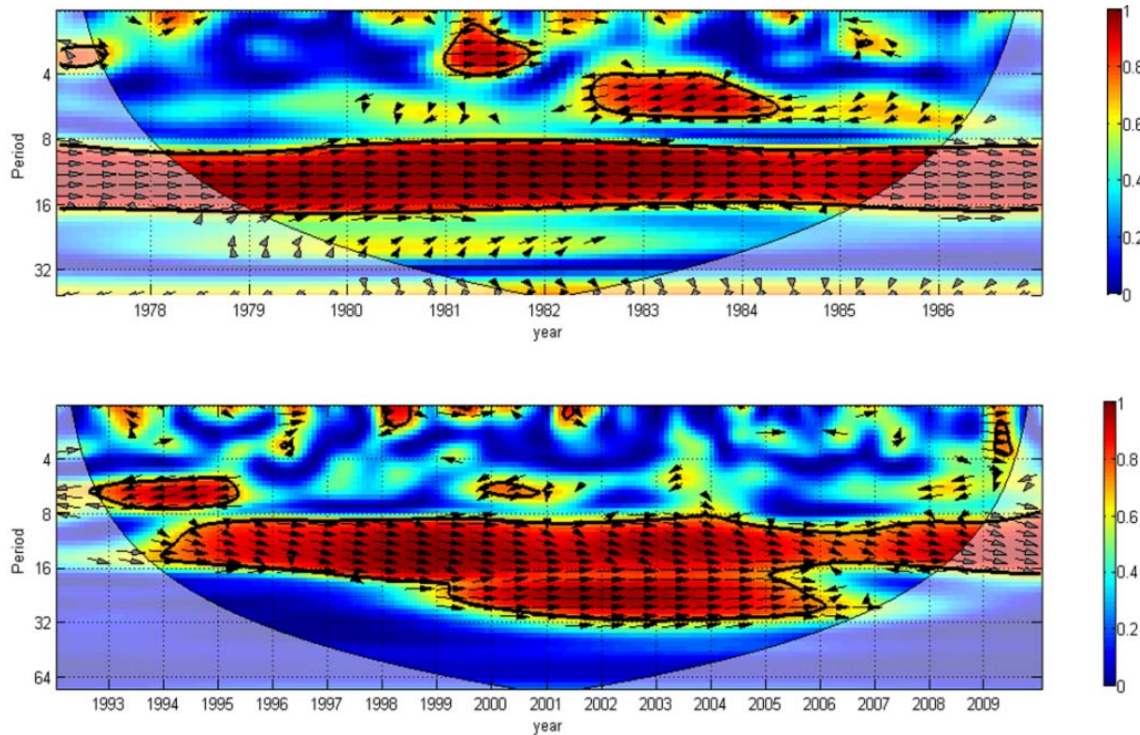


Figure 20. A result of the WTC transformation of the two signals: fire quantity FQ and factor of integral turbidity T during 1987- 1986 years (top) and 1992 – 2009 years (bottom) in Trans-Baikal region. Units of the colorbar are wavelet squared coherencies. An arrow, pointing from left to right signifies in-phase, and an arrow, pointing upward means that T series lags FQ series by 90° (phase angle is 270°).

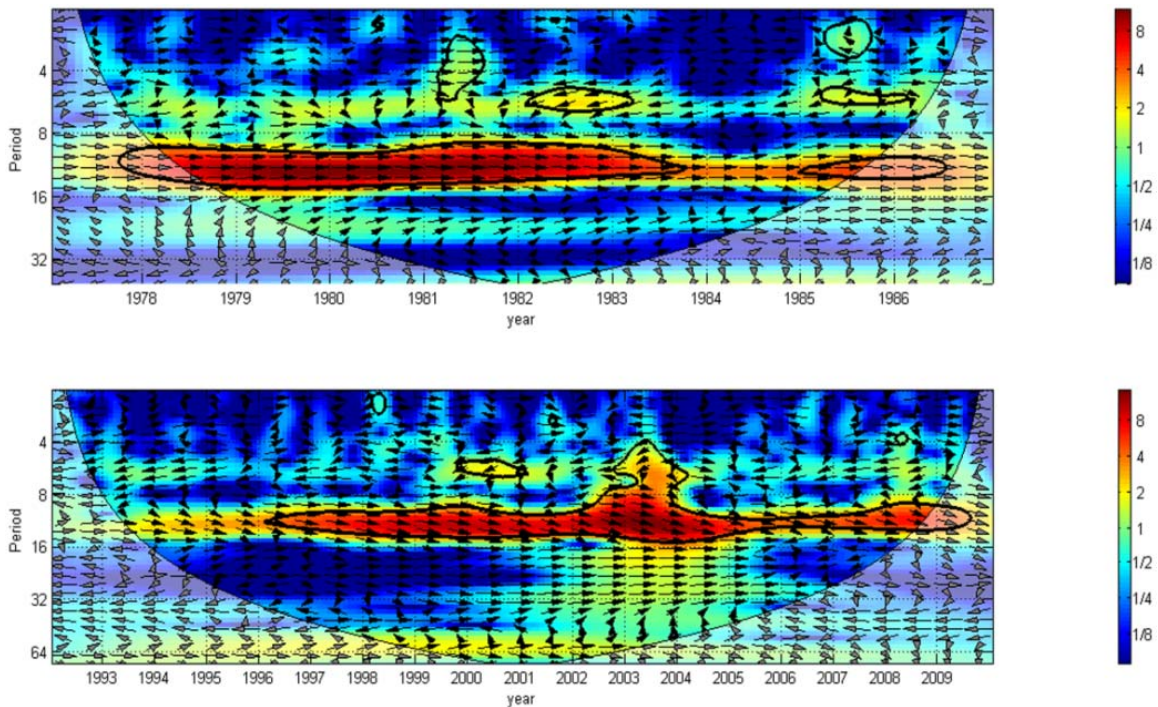


Figure 21. A result of the XWT transformation of the two signals: fire quantity FQ and factor of integral turbidity T during 1987- 1986 years (top) and during 1992 – 2009 years (bottom) in Trans-Baikal region. Units of the colorbar are wavelet squared coherencies. An arrow, pointing from left to right signifies in-phase, and an arrow, pointing upward means that T series lags FQ series by 90° (phase angle is 270°).

Notice:

The continuous WT (wavelet transformation) expands the time series into time frequency space. Cross wavelet transform (XWT) finds regions in time frequency space where the time series show high common power. Wavelet coherence (WTC) finds regions in time frequency space where the two time series co-vary (but does not necessarily have high power); See

(Grinsted et al., 2004; Jevrejeva, 2003)

9. Conclusions

The application of the AOD and T estimation technique for processing the results of observations at the Russia actinometric network stations allows obtaining qualitatively new and detailed information on the level of aerosol content of the atmosphere in separate regions and in Russia as a whole. Our analysis has made it possible to formulate the following conclusions about the spatiotemporal distribution of AOD over Russia. The spatial distribution of the AOD values averaged over the 35-year period under consideration generally corresponds to the model of global aerosol distribution over Eurasia, which is represented in the IPCC third and fourth reports. This is manifested in the AOD decrease from the southwest to the northeast in the presence of regions with continuous increasing aerosol turbidity in southwestern and southeastern Russia. Against this background, regions with increased troposphere aerosol loads are pronounced that have been more noticeable under the global purification of the atmosphere from the stratospheric aerosol layer that started in 1995. These troposphere sources are related either to an anthropogenic load (cities in southern Russia, western Siberia, and Primorskii Krai) or to forest and tundra fires in Siberia, in particular, at the Tura station in the Evenki Area. One more cause of the decreased transparency in the atmosphere over eastern Russia, which is manifested in the annual means of AOD, is the volcanoes of Kamchatka. On the whole, for Russia, the trends of multiyear variations have been negative in the last decades. However, there are stations at which the AOD trends are positive; this is particularly true of the stations of Kamchatka and the Far East. We have ascertained the peculiarities of spatial variations in the air turbidity factor in summer 2010 year in comparison with the long-term average spatial variations, which have been manifested in both distribution character and the value of the anomalies of the turbidity factor at ETR. Also we have ascertained the peculiarities of spatial and seasonal variations in the air turbidity factor T and aerosol optical depth AOD in Trans-Baikal and Central Siberia region of RF for the year and different season

The analysis of AOD variations during the last 35 years shows the following concrete estimations:

1. Total averaged AOD over all stations and the whole period under study (0.14) is very close to the annual mean global AOD value (0.14) calculated from the ECHAM-HAM model and to the estimates obtained from satellite data (0.16);
2. Maximum annual mean AOD (0.29) is reached in Krasnodar (№ 4) and the minimum one (0.07) is observed at the “aerosol pure” station of Srednekolymsk (№ 51). The

averaged special-time changes (standard deviations from the all year-averaged values of AOD for all stations) are 0.04 and are equal to mean space changes (standard deviations of mean AOD over all stations) which are found to be 0.03;

3. Minimum annual AOD values for European and Asian parts of Russia are, respectively: 0.03 and 0.02;
4. “Purification” of the atmosphere from aerosol is caused by the absence of large volcanic eruptions and by industrial “calm” conditions during the last decades. The mean AOD for the last 15 years $\{[AOD_{(1976-1994)} - AOD_{(1995-2010)}] / AOD_{(1976-2010)}\}100\%=28\%$ is lower than in the preceding 19 years. Negative tendencies are almost similar for remote and urban (as well as for rural) stations; they are less pronounced in the fall than in spring and summer;
5. Local effect of the AOD increase due to volcanic eruptions can reach 100%, while the average effects, within our consideration period, are of some percents.

Author details

Inna Plakhina

Oboukhov Institute of Atmospheric Physics, Russian Academy of Science, Russia

Acknowledgement

The study was supported by the Russian Foundation for Basic Research, project № 10-05-01086. I thank Academician G. S. Golitsyn for helpful remarks; I am helpful to my close colleague Makhotkina E.L. for her help in preparing and analysis of the experimental data.

10. References

- Abakumova, G.; Gorbarenko, E.; Chubarova, N. (2006). Estimation of Determination Accuracy of Atmosphere Aerosol Optical Thickness and Moisture Content by Data of Standart Observations on the Base of Comparison with Measurements by Solar Photometer SIMEL, Proc. of the Intern. Symp. of SNG Countries on Atmospheric Radiation MSAR-2006, 27–30 June 2006 (St.-Petersb. Gos. Univ., St.-Petersburg, 2006), pp. 43–44
- All Russia Meeting on the Status of the Air Basin in Moscow and European Russia under Extreme Weather Conditions in Summer 2010. (2010) <http://www.ifaran.ru/messaging/forum/>
- Grinsted, A.; Moore, J.; Jenrejeva, S. (2004). Application of the cross wavelet transform and wavelet coherence to geophysical time series, *Nonlinear Processes Geophys.*, 11, 561-566 (or <http://www.pol.ac.uk/research/waveletcoherence/>)
- Holben, B.; Eck, T.; Slutsker, I. et al. (1998). AERONET: a Federated Instrument Network and Data Archive for Aerosol Characterization, *Rem. Sens. Envir.* 66, 1–16

- IPCC, Climate Change (2001). Working Group I, *Contribution to the Intergovernmental Panel on Climate Change. 3rd Assessment Report Climate Change 2001: the Physical Science Basis* (Cambridge Univ., UK, New York);
http://www.grida.no/climate/ipcc_tar/wg1/166.html
- IPCC, Climate Change (2007). Working Group I, *Contribution to the Intergovernmental Panel on Climate Change. 4th Assessment Report of Climate Change: The Physical Science Basis* (Cambridge Univ., UK, New York), Ch. 2, pp. 130–234
- Isaev, A.A. (2001). *Ecological Climatology* (Naucka. Mir, Moscow, 2001)
- Jevrejeva, S., Moore, J., Grinsted, A. (2003). Influence of the Arctic Oscillation and El Niño-Southern Oscillation (ENSO) on ice conditions in the Baltic Sea: The wavelet approach, *J. Geophys. Res.*, 108(D21), 4677, doi:10.1029/2003JD003417, 2003
- Luts'ko, L.; Makhotkina, E.; Klevantsova, V. (2001). The Development of Actinometric Observations, *Current Studies of the Main Geophysical Observatory: A Jubilee Collection*, Gidrometeoizdat, St. Petersburg, pp. 184–202 [in Russian]
- Makhotkina, E.; Plakhina, I.; Lukin, A. (2005). Some Feature of Atmospheric Turbidity Change over the Russian Territory in the Last Quarter of the 20th Century. *Russian Meteorology and Hydrology*, No. 1, pp. 28 – 36, ISSN 0130 – 2906
- Makhotkina, E.; Lukin, A. Plakhina, I. (2007). Monitoring of Integral Atmosphere Transparency. *Proc. of the All-Russ. Conf. on Development of Monitoring System of Atmosphere Structure (RSMSA)* (Max Press, Moscow, 2007), p. 104
- Makhotkina, E.; Plakhina, I.; Lukin, A. (2010). Changes in Integral and Aerosol Atmospheric Turbidity in Trans-Baikal and Central Siberia. *Russian Meteorology and Hydrology*, Vol.35, No. 1, pp. 34 – 46, ISSN 1068 – 3739
- Ohmura, A. (2006). Observed Long-term Variations of Solar Irradiance at the Earth Surface. *Space Science Reviews*, Vol.125, No 1- 4, pp.111-128
- Plakhina, I.; Makhotkina, E.; Pankratova, N. (2007). Variations of Aerosol Optical Thickness of the Atmosphere in Russia in 1976-2003. *Russian Meteorology and Hydrology*, Vol. 32, No. 2, pp. 85 – 92, ISSN 1068 – 3739
- Plakhina, I.; Pankratova, N., Makhotkina, E. (2009). Variations in the Aerosol Optical Depth from the Data Obtained at the Russian Actinometric Network in 1976-2006. *Izvestiya, Atmospheric and Oceanic Physics*, Vol. 45, No. 4, pp. 456 – 466, ISSN 0001 – 4338
- Plakhina, I.; Pankratova, N., Makhotkina, E. (2011). Spatial Variations in the Air Turbidity Factor above the European part of Russia under Conditions of Abnormal Summer of 2010. *Izvestiya, Atmospheric and Oceanic Physics*, Vol. 47, No. 6, pp. 708 – 713, ISSN 0001 – 4338
- Sitnov, S. (2010). The Results of Satellite Monitoring of the Content of Trace Gases in the Atmospheric and Optical Characteristics of Aerosol over the European Territory of Russia in April–September 2010, in AllRussia Meeting on the Problem of the State of the Air Basin in Moscow and European Part of Russia under the Extreme Weather Conditions in Summer 2010 pp. 26–27, <http://www.ifaran.ru/messaging/forum/>